DOI: 10.15826/chimtech.2016.3.1.004

I. Zvereva[1*], T. Pavlova[1], V. Pantchuk[1], V. Semenov[1], Y. Breard[2], J. Choisnet[2]

[1] Institute of Chemistry, St. Petersburg State University, 198904 Petrodvorets, Saint Petersburg, Russia
[2] Laboratoire CRISMAT, UMR 6508 CNRS ENSI-CAEN and Caen University, 6 bd Maréchal Juin14050 Caen Cedex 4 France
**Corresponding author: Tel.: +7 (904) 330-50-19*
E-mail: irina.zvereva@spbu.ru

The solid solution $Sr_3Ti_{2-x}Fe_xO_{7-\delta}$ ($x \leq 0.5$): characterization of Fe (III) – Fe (IV) mixed valences**

The results of a magneto chemical and Mössbauer characterization are reported for the solid solution $Sr_3Ti_{2-x}Fe_xO_{7-\delta}$ ($x \leq 0.5$), the intergrowth of a double perovskite block and one rock-salt layer type. The charge compensation mechanism induced by the introduction of iron atoms in the matrix of $Sr_3Ti_2O_7$ is sensitive to the conditions of synthesis, namely an oxidation process triggers the formation of mixed Fe(III)–Fe(IV) valences. The crystallographic characterization - variation of the cell parameters and structure calculations – brings evidence for the respective occurrence of mixed valences and oxygen vacancies which form in the middle plane of the double perovskite block. Ferromagnetic exchange interactions which are absent in the Fe(III) containing compositions, appear and progressively strengthen depending on the oxidizing treatment. They are ascribed to the presence of an increasing amount of Fe(IV) species. Remarkably, a mixed valence state of iron forms during annealing in air with an increasing contribution of the Fe(IV) species for the larger iron contents, as deduced from Mössbauer data.

Keywords: layered oxides; solid solutions; iron; mixed valence; magnetic susceptibility; Mössbauer spectrometry.

**The authors (1) are grateful to The Russian Fund of Basic Research for its financial support (Grant 15-03-05981).

Introduction

Mixed valence states of 3d transition metals such as Ni, Co, Cu and Mn [1–7] can be stabilized in perovskite like oxides when working partial non-isovalent cationic substitutions. The fascinating electrical and magnetic properties of these oxide materials is strongly connected to the existence of these mixed valence states. Of importance to stabilize unusual oxidation degrees of 3d transition metals is the lowering of their site symmetry in the perovskite layers. In this respect the intergrowths of perovskite (P) layers and rocks-salt (RS) layers are favourable to get mixed valence states of the transition metal, whereas in the high symmetry field of the tridimensionnal perovskite structure such unusual oxidation degrees can disproportionate. In the manganites $La_{1+x}Sr_{2-x}Mn_2O_7$ with the P_2/RS intergrowth of a double perovskite block and one rock-salt layer, the existence of a colossal magnetoresistance (CMR) strongly depends on the mixed valence state of the manganese atoms [5, 6]. As to the oxygen content of these layered perovskite like phases, even if it has no concern to the oxygen stoichiometric $LnSr_2Mn_2O_7$ phases which contain Mn (III) and Mn (IV) [8], in most cases the oxygen deficiency properties are involved in the existence of the physical properties, as regularly checked in the cuprates and nickelates [1–4].

In the same way, systematic attention has been focused on the rich electrical and magnetic properties of perovskite like intergrowth structures of ferrites and their solid solutions [9–14]. As an example the existence of two P_2/RS type iron strontium mixed oxide is reported, namely the Fe(IV) one $Sr_3Fe_2O_7$ [12] and the Fe(III) one $Sr_3Fe_2O_6$ [9]. Due to this and in the frame of our previous work on P/RS type chromium doped aluminates [15] and P_2/RS chromium doped titanates [16], it was decided to look for compositions where it is possible to create mixed valence Fe(III) and Fe(IV) state of the iron atoms.

In this paper, we report on the partial substitution of iron atoms for titanium atoms in the P_2/RS type strontium titanate $Sr_3Ti_2O_7$ [17] (Fig. 1) in terms of a structural analysis (XRPD) and a magnetic and Mössbauer characterization of iron low compositions of the solid solution $Sr_3Ti_{2-x}Fe_xO_{7-\delta}$ ($x \le 0.5$). The entire solid solution exists but up to now the reported results have a concern with iron richer compositions ($2 \ge x \ge 0.5$) [18, 19]. Even more iron diluted compositions ($x \le 0.2$) were never considered for crystal chemical and physical studies, as well. Consequently, the main goal of the present work consisted in clearing up the crystal chemical mechanism of charge compensation induced by the introduction of iron atoms in the matrix of $Sr_3Ti_2O_7$: formation of the Fe (III) and Fe (IV) mixed valences together with the creation of oxygen vacancies.

Experimental

Eight compositions $Sr_3Ti_{2-x}Fe_xO_{7-\delta}$ ($0 \le x \le 0.5$) were synthesized from solid state reaction of the mixtures of precursor oxides TiO_2, Fe_2O_3 and carbonate $SrCO_3$ (Johnson Matthey, purity ≥ 99.95 %). According to the ceramics methods, the samples were pelletized and calcined in air at 1200 °C and then at 1350 °C for 40 h each.

The compositions x ≥ 0.2 were considered for X-ray structural analysis from cell parameters to structure calculations. The diluted compositions 0 < x ≤ 0.2 were retained for the magnetic and the Mössbauer study. In order to receive relevant information regarding the oxygen stoichiometry, different heating conditions were worked for some compositions as-prepared in air:

– an oxidizing treatment: 850 °C for 10 h and 150 bars oxygen pressure ($x = 0.2$ and $x = 0.5$)

– a reducing treatment: a DTA Setaram device used with an hydrogen-argon atmosphere from room temperature up to 850 °C for 8 h. This was applied specifically to the richest iron composition x = 0.5. The iron content of the as-prepared samples was determined from atomic emission spectrometry. The maximum deviation between the theoretical and the experimental value of the iron content of a given sample does not exceed 5 %.

XRPD diffractograms were recorded with a Philips PW3020 diffractometer using the Cu Kα radiation in the 2θ angular range 5–110 °, step size 0.04 ° and counting time 12s. Structure calculations were carried out with the FullProf code [20].

The magnetic susceptibility was measured according to the Faraday method in the temperature range 77–400 K. The precision is better than 2 %. Mössbauer spectra were recorded at room temperature by using spectrometer Wissel (^{57}Fe in a rhodium matrix), the isomeric shifts being calculated with respect to α Fe. In order to evaluate the part of paramagnetic species, the intensity of the signals was determined precisely up to the resonance factor.

XRPD results: cell constants and structure calculations

XRPD phase analysis ensured the existence of iron containing mixed oxide isotypic of $Sr_3Ti_2O_7$ (Fig. 1) which forms within the whole range of compositions ($0 \le x \le 0.5$). When the iron content of the $Sr_3Ti_{2-x}Fe_xO_{7-\delta}$ compositions does not exceed the value $x = 0.3$ no extra phase is observed. In the range of compositions $0.3 < x \le 0.5$ some faint amount of a $Sr_4Ti_3O_{10}$ type phase i.e. a P_3/RS intergrowth phase accompanies the major P_2/RS phase.

The values of the tetragonal unit cell constants - *a*, *c* and volume *V* for $x = 0.2$ air prepared and after oxidation, $x = 0.3$ air prepared and $x = 0.5$ (air prepared, after oxidation and after reduction) are reported in Table 1. The corresponding variation versus x is shown in Fig. 2. In order to better understand the meaning of such a variation in terms of the cru-

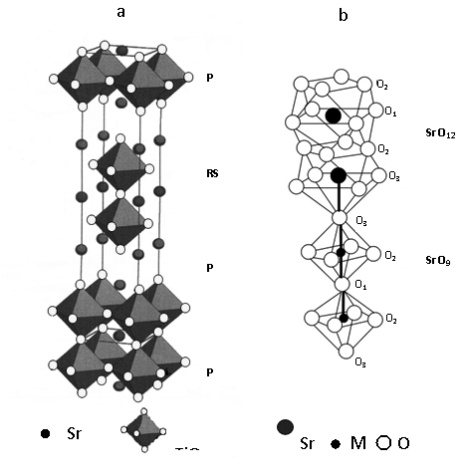

Fig. 1: (a) P_2/RS intergrowth structure of $Sr_3Ti_2O_7$: P - perovskite block; RS - rock-salt layer. (b) Connection of octahedra and MO_9 and MO_{12} polyhedra

Table 1

Unit cell parameters (Å) and volume (Å^3) in the solid solution $Sr_3Ti_{2-x}Fe_xO_{7-\delta}$

x	0 [15]	0.2 air	0.2 oxid.	0.3 air	0.5 air	0.5 oxid.	0.5 red.	*1oxid.	*1red.
a	3.902	3.8988(3)	3.8956(4)	3.8968(2)	3.8941(2)	3.8910(4)	3.8974(4)	3.877	3.898
c	20.371	20.334(4)	20.310(5)	20.323(2)	20.306(1)	20.272(5)	20.305(2)	20.26	20.20
V	310.2	309.1	308.2	308.6	307.9	306.9	308.4	304.5	307.0

*1: calculated values as the average of $Sr_3Ti_2O_7$ and $Sr_3Fe_2O_7$ (oxid.) [12] and $Sr_3Fe_2O_6$ (red.) [9].

cial problem of the mixed valences of Fe atoms, it was decided to include the variation which can be modelled in the cases of a Fe (III) and a Fe (IV) solid solution i.e. the lines which connect the oxides $Sr_3Ti_2O_7$ – $Sr_3Fe_2O_7$ and $Sr_3Ti_2O_7$ – $Sr_3Fe_2O_6$, respectively.

At first it should be stated that the nearly perfectly linear variation of V_{air} the unit cell volume of the as-prepared compositions (Fig. 2a) brings evidence for the existence of a solid solution in the entire range of compositions $0 \le x \le 0.5$. Moreover the variation of V strongly depends on the heating conditions: the oxidized compositions – Fe (IV) – exhibit a value of V_{ox} smaller than the reduced one V_{red} – Fe (III) whereas V_{air} takes intermediate values. More precisely, the latter result is the combination of two different trends in the crystal chemical evolution of the solid solution $Sr_3Ti_{2-x}Fe_xO_{7-\delta}$ herein investigated:

– in the oxidized compositions, the substitution of the smaller Fe^{4+} cations (r_{CNVI} = 0.585 Å) [21] for the Ti^{4+} one (r_{CNVI} = 0.605 Å) results in a decrease of V.

– in the reduced compositions, the creation of oxygen vacancies cancels the effect of the substitution of bigger Fe^{3+} cations (r_{CNVI} = 0.645 Å) for the Ti^{4+} one, resulting in an overall decrease of V whose slope is weaker than in the oxidized compositions.

The precise contribution of *a* (Fig. 2b) and *c* (Fig. 2c) parameters to the variation of the unit cell volume is rather difficult to ensure. At least one can assume the parameter *a* to be more sensitive to the decrease of size of the cations sitting in the octahedral sites. This result fully agrees with that is reported in the study of the compositions $x \ge 0.5$ i.e. annealing at high oxygen pressure triggers a decrease

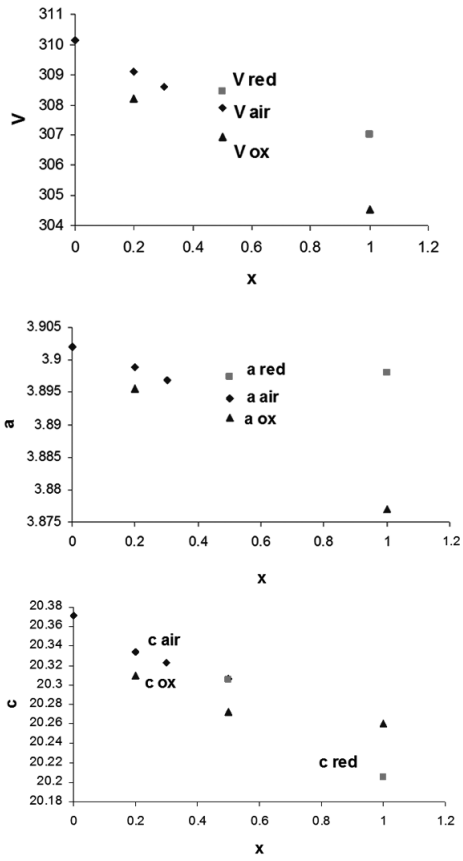

Fig. 2: Variation of the cell volume (Å^3) and cell parameters (Å) in the solid solution $Sr_3Ti_{2-x}Fe_xO_{7-\delta}$

of the parameter *a* [19]. On the contrary, the existence of a large amount of oxygen vacancies induces a pronounced lowering of the value of the parameter *c*.

As a main result of the observed variation of the unit cell volume, it must be stated that the solid solution $Sr_3Ti_{2-x}Fe_xO_{7-\delta}$ which forms by heating in air contains a mixed valence state of the iron atoms. In order to learn about some modifications which are expected in the P_2/RS intergrowth of the iron containing solid solution, it was decided to carry out a profile analysis of the XRPD difractograms of the compositions $x \geq 0.2$. For $x = 0.5$ three cases were considered: as-prepared in air, oxidized and reduced samples and for x = 0.2 the as-prepared and the oxidized sample. The structure of $Sr_3Ti_2O_7$ [17] was retained: S.G. I4/mmm. Concerning the oxygen non-stoichiometry, XRPD is rather unsensitive to a small variation of the oxygen content. Consequently, only in a final step of the calculations of the air prepared compositions, a value of δ the oxygen deficiency arbitrarily fixed to the half of the maximum value corresponding to a full reduction was considered ($\delta = x/4$). The results of the Mössbauer characterization here after reported ensured a value of δ close or lower than the half of a full reduction. As it was previously performed in the chromium containing solid solution $Sr_3Ti_{2-x}Cr_xO_{7-\delta}$ [16] we did an attempt to find the likely location of the oxygen vacancies in one of the three possible sites, namely the inner apical O_1, the equatorial O_2 and the outer apical O_3 (Fig. 1b). In this respect, the main results to be received from the structural analysis are as follows:

– the oxygen deficiency of the air prepared and reduced compositions occurs in the inner apical O_1 positions i.e. in the middle plane of the double perovskite block. This meets the different data obtained in the P_2/RS cuprates [22] and the solid solution $Sr_3Ti_{2-x}Cr_xO_{7-\delta}$ [16].

– the equatorial M-O_2 distances (Table 2), within the precision of the calculation procedure are unsensitive to the substitution of iron atoms for titanium.

– as regularly observed in the intergrowth structures, there is an apical distorsion of the octahedra, as visible from the obtained values of the corresponding inner apical M-O_1 and outer apical M-O_3 distances (Table 2). The main data observed in $Sr_3Ti_2O_7$ i.e. the coupling of a longer inner M-O_1 distance with a smaller outer M-O_3 one is saved for the whole series of compositions.

Table 2

Metal oxygen distances (Å) in the (Ti, Fe)O_6 octahedra in the solid solution $Sr_3Ti_{2-x}Fe_xO_{7-\delta}$

M-O dist. M = Ti, Fe	$Sr_3Ti_2O_7$ Air prep.[17]	$x = 0.2$ Oxidized	$x = 0.2$ Air prep.	$x = 0.3$ Air prep.	$x = 0.5$ Oxidized	$x = 0.5$ Air prep.	$x = 0.5$ Red.
M-O_1 x1	1.995	2.02(1)	2.02(1)	2.00(1)	2.03(1)	2.00(1)	2.02(1)
M-O_2 x4	1.949	1.95(1)	1.95(1)	1.95(1)	1.95(1)	1.95(1)	1.95(1)
M-O_3 x1	1.887	1.91(2)	1.92(2)	1.94(2)	1.91(2)	1.91(2)	1.96(2)

Magneto chemical and mossbauer results

The temperature dependence of the molar magnetic susceptibility in four air prepared compositions (x = 0.02; 0.08; 0.12; 0.18) of the solid solution

$Sr_3Ti_{2-x}Fe_xO_{7-\delta}$ is shown in Fig.3. Within the temperature range 77–400 K there is a monotonic decrease of χ versus T and for given temperature the observed value of χ systematically increases when x, the iron content, gets larger. The experimental data of the molar magnetic susceptibility have been used for calculating a paramagnetic value per one mole of iron, by subtracting the diamagnetic contribution of $Sr_3Ti_2O_7$ and iron atoms. The thermal variation of the paramagnetic susceptibility is described by a Curie-Weiss law $\chi = C/(T-\theta)$ over the whole temperature range under consideration. Curie constant C takes a value close to 4 emu.K, where as Weiss temperature θ, slightly increases versus *x* (Table 3).

Table 3

Curie constant C and Weiss temperature θ in the air prepared) $Sr_3Ti_{2-x}Fe_xO_{7-\delta}$

x	C, emu.	θ, K
0.02	4.07	-18
0.08	4.00	-1.1
0.12	4.04	2.8
0.18	4.01	7.8

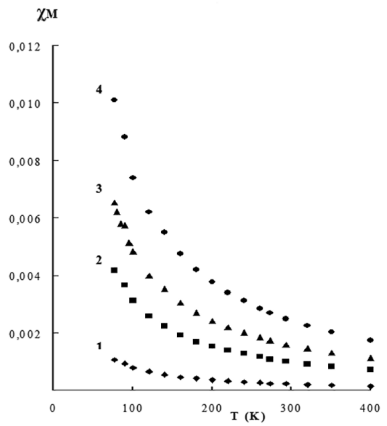

Fig. 3. Temperature dependence of χ_M the molar magnetic susceptibility for the air prepared solid solution $Sr_3Ti_{2-x}Fe_xO_{7-\delta}$. 1. $x = 0.02$; 2. $x = 0.08$; 3. $x = 0.12$;4. $x = 0.18$

The calculated effective magnetic moment μ_{eff} shows a complex dependence on both temperature and iron content, as visible in Fig. 4 for the air prepared compositions $x = 0.02, 0.08; 0.12; 0.18$. Such behaviour cannot be explained on the basis of one paramagnetic species and consequently, a mixed valence state of the iron cations which are introduced in the diamagnetic matrix of $Sr_3Ti_2O_7$ is likely to occur in the solid solution. Concerning the magnetic interactions, it can be reasonably assumed that they progressively change from an antiferromagnetic property to a ferromagnetic one, depending on an increasing of iron content.

The concentration dependence of μ_{eff} in the temperature range 298–400 K can be modelled in the following way:

$$\mu_{298K} = 5,44 + 2,11x$$
$$\mu_{400K} = 5,47 + 1,82x \quad (1)$$

By extrapolating these equations at zero concentration of iron, the value of the effective magnetic moment $\mu_{x\to 0}$ of a single iron cation in the solid solution above the room temperature (RT) can be estimated as nearly constant and equal to 5.45 MB.

The theoretical values of μ_{eff} of a single iron cation are 5.92 MB and 4.9 MB, for Fe^{3+} (s = 5/2) and Fe^{4+} (s = 2), respectively. Clearly, the observed value 5.45 MB gives evidence for the presence of iron cations with a number of unpaired electrons smaller than 5, very likely 4 as in the Fe^{4+} species. If the exchange interactions between the paramagnetic iron species above RT are assumed to be weak enough not to induce a deviation of the effective magnetic moment with respect to the value of μ_{eff} for a single paramagnetic iron

cation, the existence of a Fe(III)-Fe(IV) mixed valence state of the iron atoms in the solid solution is ensured.

The observed effective magnetic moment in the solid solution with a zero concentration of iron can be modelled in terms on the only Fe^{3+} and Fe^{4+} cations, according to the following formula:

$$\mu^2_{x\to 0} = 0_{Fe^{3+}}\mu^2_{Fe^{3+}} + a_{Fe^{4+}}\mu^2_{Fe^{4+}}$$
$$a_{Fe^{3+}} + a_{Fe^{4+}} = 1 \qquad (2)$$

where μ_i and a_i are the magnetic moment and the concentration of a given iron cation. Introducing into this equation the calculated value of $\mu_{x\to 0}$ = 5.45 MB allows to calculate the concentration of Fe^{4+} as equal to 0.48(4). The presence of the two species Fe^{3+} and Fe^{4+} in the diluted solid solution looks unambiguous.

Considering the temperature dependence of the effective magnetic moment allows to point to the following statements:

– for the lowest iron concentrations ($x \le 0.08$) the magnetic properties, up to a large extent, correspond to what is expected from antiferromagnetic exchange interactions.

– for larger iron concentrations ($x > 0.08$) ferromagnetic exchange interactions take an increasing part depending on an increasing iron concentration (Fig. 4).

The Fe(III) – Fe(IV) mixed valence state of the iron atoms in the solid solution triggers three kinds of magnetic exchange interactions, namely Fe^3-O-Fe^{3+}, Fe^{3+}-O-Fe^{4+} et Fe^4-O-Fe^{4+}. Exchange interactions between Fe^{3+} cations in the layered perovskite like phases are antiferromagnetic [23, 24]. When atoms with different electronic configuration are concerned, the exchange interactions are always ferromagnetic. As regards the Fe^{4+}-O-Fe^{4+} exchange interactions, they are either antiferromagnetic or ferromagnetic depending on the site symmetry of the iron atoms. In order to learn about the character of the exchange interactions in the Fe^{4+}-O-Fe^{4+} clusters, an analysis of the influence of the experimental heating conditions on the magnetic properties was carried out in the limiting composition x = 0.5 of the solid solution. The tempera-

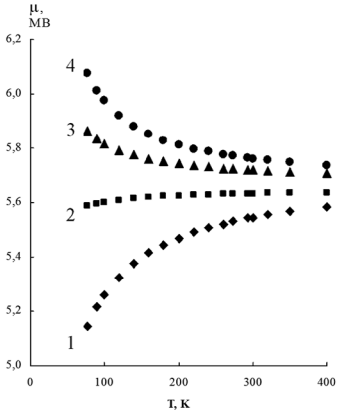

Fig. 4. Variation of the effective magnetic moment versus temperature in the air prepared solid solution $Sr_3Ti_{2-x}Fe_xO_{7-\delta}$. 1. x = 0.02; 2. x = 0.08; 3. x = 0.12; 4. x = 0.18

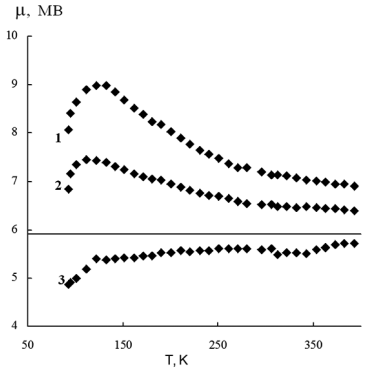

Fig. 5: Variation of the effective magnetic moment versus temperature in the composition x = 0.5. 1. oxidizing treatment; 2. air prepared; 3. reducing treatment; ––: single Fe^{3+} cation

ture dependence of the effective magnetic moment observed in $Sr_3Ti_{1.5}Fe_{0.5}O_{7-\delta}$ as prepared in air and heated in oxidizing or reducing conditions, is shown in Fig. 5. In the latter case, the sample contains only Fe^{3+} species, as checked by thermal analysis, and the exchange interactions are antiferromagnetic. Above RT (Fig. 6) μ_{eff} in the reduced sample takes a value very similar to that of the Fe^{3+} cation 5.92 MB. In the air prepared sample the value of μ_{eff} is intermediate between the reducing and the oxidizing cases, which result ensures the existence of two different exchange interactions. Finally, in the oxidized sample the Fe^{4+} species are responsible of the strong ferromagnetic character of the exchange interactions, in agreement with the results reported for the ferrate $Sr_3Fe_2O_7$ [12].

At this stage, one result remains not immediately understandable in a simple way: the value of μ_{eff} even at temperatures higher than RT (Fig. 5) largely exceeds the value of single Fe^{4+} cations: approximately 7 MB to be compared with 4.9 MB. One must take into account that for such iron concentration in the solid solution (25 %) the tendency of the paramagnetic species to aggregate will be important. It was previously observed and modelled in the P/RS intergrowth structure of the solid solution $YCaAl_{1-x}Cr_xO_4$ [25]. Consequently, the actual value of the magnetic moment will be due not only to the single monomeric iron species but it will include the contribution of the various clusters, at least up to tetramers which likely have a concern to the observed magnetic moment.

As deduced from the temperature dependence of the effective magnetic moment, the ferromagnetism of the exchange interactions undoubtedly increases versus the increasing amount of iron in the solid solution. More precisely, this data gives evidence for the increasing part of the Fe^{4+} species. In order to receive another evidence for the presence of Fe^{4+} and even more to calculate its concentration, the solid solution was studied by Mössbauer spectrometry. Fig. 6 shows Mössbauer spectra of three compositions

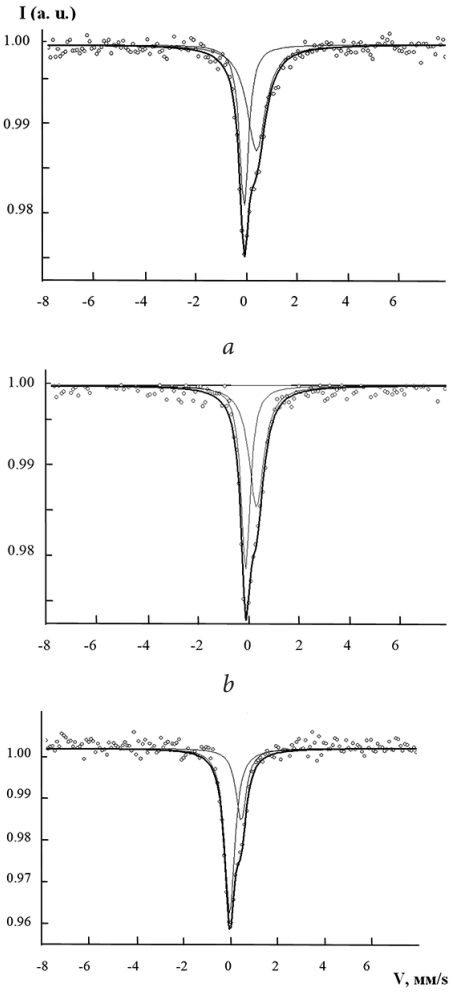

Fig. 6. Mössbauer spectra of air prepared compositions of the solid solution $Sr_3Ti_{2-x}Fe_xO_{7-\delta}$: *a* – 0.12; *b* – 0.16; *c* – 0.2

x = 0.12; 0.16; 0.20 prepared in air. In any case there is the superposition of two signals with very different isomeric shifts δ_1 = 0.431 mm/s and δ_2 = –0.08 mm/s – corresponding to the cations Fe^{3+} and Fe^{4+}, respectively [26–28]. The observed value of the quadrupolar splitting for Fe^{3+} ΔE_1 = 0.29 mm/s - is consistent with a lower site symmetry for Fe^{3+} than for Fe^{4+} ΔE_2 = 0.22 mm/s. On the basis of the Jahn-Teller effect of the $3d^4$ Fe^{4+} cations, a supplementary distortion of the corresponding ($Fe^{4+}O_6$) octahedra is expected. In fact, the existence of oxygen vacancies in the inner apical positions of the double perovskite block, as ensured from the structure calculations, triggers a lowering of the site symmetry of the Fe^{3+} cations.

For comparison, the solid solution $Sr_{3-x}La_xTi_{2-x}Fe_xO_7$ was considered. In such case the fully charge compensated double substitution of the cationic couple x (La^{3+} + Fe^{3+}) for x (Sr^{2+} + Ti^{4+}) allows to maintain the oxygen stoichiometry i.e. there are no oxygen vacancies. The Mössbauer data observed for the composition x = 1 namely $Sr_{2.9}La_{0.1}Ti_{1.9}Fe_{0.1}O_7$ reveal the existence of one signal with an isomeric shift δ = 0.32 mm/s which corresponds to an iron cation Fe^{3+} in a high symmetry local field. Clearly, this is another proof that the Mössbauer spectrometry ensures the presence of the two species Fe^{3+} and Fe^{4+} in the air prepared solid solution $Sr_3Ti_{2-x}Fe_xO_{7-\delta}$.

The analysis of the iron concentration dependence of the intensity of the two Mössbauer signals brings the opportunity to evaluate the respective parts of Fe^{3+} and Fe^{4+}. In Table 4 we report for the three compositions x = 0.12; 0.16; 0.20 the estimated values of the Fe^{3+} and Fe^{4+} concentration (%) and the corresponding values of y the (Fe^{4+}) composition and δ the oxygen deficiency.

Table 4

Fe^{4+} and Fe^{3+} concentration (%), y (Fe^{4+}) composition and estimated value of δ the oxygen deficiency in the solid solution $Sr_3Ti_{2-x}Fe_xO_{7-\delta}$ (air prepared)

x	Fe^{4+}(%)	Fe^{3+}(%)	y (Fe^{4+})	δ
0.12	41.5	58.5	0.05	0.035
0.16	46.7	53.3	0.07	0.045
0.20	66.5	33.5	0.13	0.035

We receive the confirmation that the amount of Fe^{4+} increases versus x the iron composition i.e. when the iron concentration in the solid solution is large enough - $x \geq 0.16$ - the air prepared samples contain the Fe^{4+} cations as main species. These results are in good agreement with the main information obtained from the magnetic properties. Finally an estimation of δ the oxygen deficiency in the solid solution $Sr_3Ti_{2-x}Fe_xO_{7-\delta}$ allows to ensure the oxygen non-stoichiometry property which is not large enough ($\delta < x/4$) to be determined from XRPD calculations.

Conclusion

The solid solution $Sr_3Ti_{2-x}Fe_xO_{7-\delta}$ within its homogeneity range shows a remarkable ability to promote an oxidation of Fe(III) to Fe(IV) even annealed in air. The existence of a mixed valence state of the iron atoms with a major contribution of the Fe(IV) species is well established. In this respect, these new data well compare with those previously obtained in the case of chromium atoms in the solid solution $Sr_3Ti_{2-x}Cr_xO_{7-\delta}$ [16]. In both cases the significant trend to get Fe(Cr)(IV) species

mainly results from the weak ability of these substituted titanates to tolerate the formation of oxygen vacancies in the middle plane of the double perovskite block. In this way, their crystal chemical properties are closer to that of the manganites $La_{1+x}Sr_{2-x}Mn_2O_7$ [8] than the cuprates $La_{2-x}Sr(Ca)_xCu_2O_{6-x/2+\delta}$ [20]. In the latter case, the middle plane of the double perovskite block is fully deprived of oxygen atoms.

1. Nguyen N., Choisnet J., Hervieu M., Raveau B. Oxygen defect K_2NiF_4-type oxides: The compounds $La_{2-x}Sr_xCuO_{4-x/2+\delta}$. *J. Solid State Chem.* 1981;39:120-127. doi:10.1016/0022-4596(81)90310-8
2. Ando Y., Sera M., Yamagata S., Kondoh S., Onoda M., Sato M. Normal state properties of $La_{2-x}Sr_xCuO_4$ and $La_2SrCu_2O_y$. *J. Solid State Comm.* 1989;70:303-308. doi:10.1016/0038-1098(89)90332-3
3. Kakol Z., Spalek J., Honig J. M. Superconductivity and antiferromagnetism in $La_{2-}xSrxNiO_4$ *J. Solid State Chem.* 1989;79:288-292. doi:10.1016/0022-4596(89)90277-6
4. Manthiram A., Tang J. P., Manivannan V. Factors Influencing the Stabilization of Ni+ in Perovskite-Related Oxides. *J. Solid State Chem.* 1999;148:499-507. doi:10.1006/jssc.1999.8487
5. Seshadri R., Martin C., Maignan A., Hervieu M., Raveau B., Rao C. N. R. Structure and magnetotransport properties of the layered manganites $Re_{1.2}Sr_{1.8}Mn_2O_7$(RE = La, Pr, Nd). *J. Mater. Chem.* 1996;6:1585-1590. doi: 10.1039/JM9960601585
6. Battle P. D., Rosseinsky M. J. Synthesis, structure, and magnetic properties of $n = 2$ Ruddlesden–Popper manganates. *Current Opinion in Solid State and Materials Science.* 1999;4: 163-170. doi:10.1016/S1359-0286(99)00012-1
7. Volkova N. E., Kolotygin V. A., Gavrilova L. Ya., KhartonV. V., Cherepanov V. A. Nonstoichiometry, thermal expansion and oxygen permeability of $SmBaCo_{2-x}Cu_xO_{6-\delta}$ *Solid State Ionics.* 2014;260:15-20. doi:10.1016/j.ssi.2014.03.003
8. Battle P. D., Green M. A., Laskey N. S., Millburn J. E., Murphy L., Rosseinsky M. J., Sullivan S. P., Vente J. F. Layered Ruddlesden−Popper Manganese Oxides: Synthesis and Cation Ordering. *Chem. Mater.* 1997;9:552-559. doi: 10.1021/cm960398r.
9. Dann S. E., Weller M. T., Currie D. B. Structure and oxygen stoichiometry in $Sr_3Fe_2O_{7-y}$, $0 \le y \le 1.0$. *J. Solid State Chem.* 1992;97:179-185. doi:10.1016/0022-4596(92)90023-O
10. Lee J. Y., Swinnea J. S., Steinfink H., Reiff W. M. The Crystal Chemistry and Physical Properties of the Triple Layer Perovskite Intergrowths $LaSr_3Fe_3O_{10-\delta}$ and $LaSr_3(Fe_{3-}xAlx)O_{10-\delta}$. *J. Solid State Chem.* 1993;103:1-15. doi:10.1006/jssc.1993.1072
11. Prado F., Manthiram A. Synthesis, Crystal Chemistry, and Electrical and Magnetic Properties of $Sr_3Fe_{2-x}Co_xO_{7-\delta}$ ($0 \le x \le 0.8$). *J. Solid State Chem.* 2001;158:307-314. doi:10.1006/jssc.2001.9111
12. Mori K., Kamiyama T., Kobayashi H., Torii S., Izumi F., Asano H. Crystal structure of $Sr_3Fe_2O_{7-\delta}$. *J. Phys. Chem. Solids.* 1999;60:1443-1446. doi:10.1016/S0022-3697(99)00158-4

13. Ghosh S., Adler P. Competing magnetic interactions and large magnetoresistance effects in a layered iron(IV) oxide: citrate–gel synthesis and properties of $Sr_3Fe_{1.8}Co_{0.2}O_{\sim 7}$. *Solid State Com.* 2000;116:585-589. doi:10.1016/S0038-1098(00)00400-2
14. Hodges J. P., Short S., Jorgensen J. D., Xiong X., Dabrowski B., Mini S. M., Kimball C. W. Evolution of Oxygen-Vacancy Ordered Crystal Structures in the Perovskite Series $Sr_nFe_nO_{3n-1}$ (n = 2, 4, 8, and ∞), and the Relationship to Electronic and Magnetic Properties. *J. Solid State Chem.* 2000;151:190–209. doi:10.1006/jssc.1999.8640
15. Zvereva I., Zueva L., Archaimbault F., Crespin M., Choisnet J., Lecompt J. Crystallochemical, magnetic and electrical properties of the K_2NiF_4 type diluted solid solutions $Y_{0.9}Ca_{1.1}Cr_yAl_{1-y}O_4$ (y≤0.10): evidence for a partial Cr^{+3}→Cr^{+4} oxidation. *Materials Chemistry and Physics.* 1997;48:103-110. doi:10.1016/S0254-0584(97)80102-2
16. Zvereva I., German I., Smirnov Yu., Choisnet J. Evidence of Cr^{+4} doping in $Sr_3Ti_2O_7$ from structural, optical and magnetic properties. *J. Mat. Sci. Letters* 2001 ;20 :127-130. doi:10.1023/A:1006786119155
17. Ruddlesden S. N., Popper P. The compound $Sr_3Ti_2O_7$ and its structure. *Acta Crystallogr.* 1958;11:54-55. doi: 10.1107/S0365110X58000128
18. Adler P. Charge disproportionation in iron(IV) oxides: electronic properties and magnetism in $Sr_3Fe_{2-x}Ti_xO_{7-y}$ annealed at high oxygen pressures. *J. Mater. Chem.* 1999;9:471477. doi: 10.1039/A806772D
19. Shilova Y., Patrakeev M., Mitberg E., Leonodov I., Kozhevnikov V., Poeppelmeier K. Order–Disorder Enhanced Oxygen Conductivity and Electron Transport in Ruddlesden–Popper Ferrite-Titanate $Sr_3Fe_{2-x}Ti_xO_{6+\delta}$. *J. Solid State Chem.* 2002;168:275-283. doi:10.1006/jssc.2002.9722
20. Rodriguez-Carvajal J. L. Recent advances in magnetic structure determination by neutron powder diffraction. *Physica B.* 1993;192:55-69. doi:10.1016/0921-4526(93)90108-I
21. Shannon D. D. Revised effective ionic radii and systematic studies of interatomic distances in halides and chalcogenides. *Acta Cryst A*. 1976;32:751-767. doi: 10.1107/S0567739476001551
22. Nguyen N., Er-Rakho L., Michel C., Choisnet J., Raveau B. Intercroissance de feuillets "perovskites lacunaires" et de feuillets type chlorure de sodium: Les oxydes $La_{2-x}A_{1+x}Cu_2O_{6-x/2}$ (A = Ca, Sr). *Mat. Res. Bull.* 1980;15:891-897. doi:10.1016/0025-5408(80)90212-3
23. Soubeyroux J., Courbin P., Fournes L., Fruchart D., Le Flem G. La phase $SrLaFeO_4$: Structures cristalline et magnétique. *J. Solid State Chem*. 1980;31:313-320. doi:10.1016/0022-4596(80)90093-6
24. Sharma I. B., Singh D., Magotra S. K.. Effect of substitution of magnetic rare earths for La on the structure, electric transport and magnetic properties of $La_2SrFe_2O_7$. *J. of Alloys and Compounds***.** 1998;269:13–16. doi:10.1016/S0925-8388(98)00153-4
25. Archaimbault F., Choisnet J., Zvereva I.. Crystal chemistry and magnetic properties of the K_2NiF_4 type diluted solid solution $YCaAl_{1-x}Cr_xO_4$ ($0 \leqslant x \leqslant 0.10$): evidence for Cr^{3+}. *Mat. Chem. Physics.* 1993;34:300-305. doi:10.1016/0254-0584(93)90051-M

26. Kobayashi H., Kira M., Onodera H., Suzuki T., Kanimura T. Electronic state of $Sr_3Fe_2O_{7-y}$ studied by specific heat and Mössbauer spectroscopy. *Physica B.* 1997;237:105-107. doi:10.1016/S0921-4526(97)00065-3
27. Shilova A., Chislova I., Panchuk V., Semenov V., Zvereva I. Evolution of iron electronic state in the solid solutions $Gd_{2-x}Sr_{1+x}Fe_2O_{7-\delta}$. *Solid State Phenomena.* 2013;194:116-119. doi:10.4028/www.scientific.net/SSP.194.116
28. Al-Rawas A. D., Widatallah H. M., Al-Harthi S. H., Johnson C., Gismelseed A. M., Elzain M. E., Yousif A. A. The formation and structure of mechano-synthesized nanocrystalline $Sr_3Fe_2O_{6.4}$: XRD Rietveld, Mössabuer and XPS analyses. *Mat. Res. Bull.* 2015;65:142-148. doi:10.1016/j.materresbull.2015.01.026